LA-UR-16-28191
Approved for public release; distribution is unlimited.

Title: Benchmarking PARTISN with Analog Monte Carlo: Moments of the Neutron Number and the Cumulative Fission Number Probability Distributions

Author(s): O'Rourke, Patrick Francis

Intended for: Report

Issued: 2016-10-27

LA-UR-15-?????

Los Alamos NATIONAL LABORATORY EST.1943

# memorandum

*Computer and Computational Sciences*
*Computational Physics and Methods, CCS-2*

*To/MS:* Distribution
*From/MS:* Patrick F. O'Rourke
*Phone/FAX:* 7-1476
*Symbol:* CCS-2:16-041
*Date:* October 20, 2016

**Subject: Benchmarking PARTISN with Analog Monte Carlo: Moments of the Neutron Number and the Cumulative Fission Number Probability Distributions**

## 1 Introduction

The purpose of this report is to provide the reader with an understanding of how a Monte Carlo neutron transport code was written, developed, and evolved to calculate the probability distribution functions (PDFs) and their moments for the neutron number at a final time as well as the cumulative fission number, along with introducing several basic Monte Carlo concepts. The primary motivation for writing an analog Monte Carlo neutron transport code is to benchmark the recently implemented capabilities for calculating the moments of the neutron population and the cumulative fission numbers using deterministic transport methods into LANL's PARTISN code [1] (PARallel, TIme-dependent $S_N$). The capstone version of the MC code is to simulate spherical multiplying systems that are time-dependent with multigroup neutrons to calculate the neutron number PDF and the cumulative fission PDF and the respective moments for those PDFs, addressing the concerns stated below and bringing to light the vast validity of one of PARTISN's newest capabilities.

Although MCATK would initially be the MC code of choice for calculating the moments of the neutron population [2], it will prove to be an insufficient benchmarking tool as it treats the energy-dependent neutron cross-sections continuously [3] while PARTISN solves the neutron transport equations for the moments using multigroup energy discretization [4]; the difference in the handling of the continuous energy versus the multigroup data has, and will, undoubtedly lead to discrepancies. The final section of this report describes the extension of the spherical time-dependent MC code to account for, and utilize, multigroup neutron cross-sections as a means to more accurately simulate the physics that PARTISN represents.

Also of concern is the validity of utilizing deterministic transport methods to characterize systems by their moments in which the neutron population behaves unpredictably. In strongly stochastic systems where the neutron population is small and can vary considerably depending on the persistence of any individual fission chain, the magnitude of the population may fluctuate orders of magnitude from one instance to the next. The PDFs and their higher order moments must be considered for such systems where the mean of the population is not truly representative of the actual population. Several elements of the systems of interest that introduce stochasticity into the neutron population include, but are not exhausted by, particle multiplicity emission from fission events (both induced and spontaneous); weak, randomly emitting sources or cosmic radiation; low populations for which fission chains do not physically overlap and are well-separated in time; the temporal propagation of any individual fission chain, which could be short-lived or could ultimately lead to a criticality excursion.

The outline of the document is now disclosed. Section 2 is a verification of the most simple form the MC code takes in generating the neutron number and cumulative fission number PDFs: a time-dependent lumped (PDFs are not functions of space, angle, nor energy) system with monoenergetic neutrons. The temporal sampling techniques are compared against several analytically derived solutions to the forward master equations for different initial conditions, source strengths, final times, multiplicity models, and special neutron interaction scenarios. Section 3 is a further extension of the time-dependent MC code into one-dimensional slab systems, of which we begin the benchmarking trails on PARTISN. As PARTISN directly calculates the moments of the PDFs, this is the primary comparison made with the MC, and as an extra, the actual PDFs from the MC are plotted. Next, Section 4 is similar to Section 3, except it compares the spherical time-dependent one-group MC code to PARTISN. Finally, Section 5 further extends the spherical time-dependent MC code to include multigroup capabilities.

## 2 Time-Dependent Lumped Systems

This section is concerned with comparing the probability distribution functions (PDFs) calculated by the Monte Carlo code with analytical expressions for several scenarios.

Most time-dependent analytical expressions can only be obtained for lumped systems (probabilities are not functions of space, energy, or angular variables) using a forward-in-time probability balance of all the mutually exclusive events a neutron may experience that will contribute to a final state of the system. The reasoning for doing so is to ensure that the MC program is simulating the temporal variable correctly before we may confidently incorporate spatial and energy dependence.

All of the following analytical expressions (except for the Poisson Distribution) are obtained by enforcing a binary induced fission model (BIF), where two and only two neutrons are emitted in every induced fission, along with restricting singlet-emitting source events (SS) with the possibility of there existing zero (0) or one (1) neutron at the initial time; the combination of these two emission distributions is called the Binary Fission Model (BFM). The primary material and neutron properties are summarized in Table (1) and are constant throughout the ensuing lumped model simulations unless otherwise stated.

| $N$ | $v$ | $T_{1/2}$ | $p_{SF}$ |
|---|---|---|---|
| $5.00 \cdot 10^{-2}\ (cm * b)^{-1}$ | $2.02 \cdot 10^{9}\ cm/s$ | $7.608 \cdot 10^{11}\ s$ | $4.4 \cdot 10^{-12}$ |

**Table 1:** Data set for the simulated material.

The three primary mutually exclusive interactions that influence the neutron population in a multiplying system are source emission by spontaneous fission (SF), induced fission, and parasitic absorption. A balance of the probabilities of possible interactions can be constructed utilizing the Markov property of nuclear reactions (i.e., particles possess no memory of their origin). This probability balance can be algebraically manipulated and, taking the time limit, is converted into a system of ordinary differential equations collectively known as the forward differential Chapman-Kolmogorov equation or more commonly as the forward master equation of the neutron PDF

$$\begin{aligned}\frac{\mathrm{d}P_n(t)}{\mathrm{d}t} =& -(\lambda_a n + S)P_n(t) + \lambda_c(n+1)P_{n+1}(t) \\ &+ S\sum_{\nu=0}^{\nu_m^S} q_\nu^S P_{n-\nu}(t) + \lambda_f \sum_{\nu=0}^{\nu_m^f} q_\nu^f (n-\nu+1)P_{n-\nu+1}(t),\end{aligned} \tag{1}$$

where $n = 0, 1, 2, \ldots$. The general initial condition is given by the Kronecker delta function as

$$P_n(t=0) = \delta_{n,n'} = \begin{cases} 1 & \text{for } n = n' \\ 0 & \text{for } n \neq n'. \end{cases} \tag{2}$$

In Eq. (1), $\lambda_a$ , $\lambda_c$ , and $\lambda_f$ are the absorption, capture, and fission reaction rates of the neutrons, $S$ is the SF source strength, i.e., the probability per unit time of a source event occurring, $q_\nu^{S/f}$ are the neutron multiplicity distributions for source and fission events, $\nu_m$ are the maximum number of neutrons emitted in either the source or fission events (note that the values are not equal to each other between the two summations and are dependent on the system's isotopic composition). Noting the the reaction rate for interaction $x$ can be determined as $\lambda_x = p_x/\tau = \sigma_x/(\sigma_a \tau)$, we can readily determine the reaction rates from the material's microscopic cross sections, $\sigma$, and the neutron lifetime, $\tau = 1/(v\Sigma_a)$, in a lumped system ($v$ is the neutron speed and $\Sigma_a$ is the macroscopic absorption cross section).

For a given system mass $m$, the SF source, $S$, can be determined by summing the individual contributions of all spontaneous fissioning isotopes, $i$:

$$S = mN_A \sum_i \frac{p_{SF,i}\lambda_i w_i}{M_i}, \tag{3}$$

where $N_A$ is Avogadro's Constant, $p_{SF,i}$ is the probability that a radioactive decay of isotope $i$ is a spontaneous fission event, $\lambda_i$ is the decay constant of $i$, $w_i$ is the weight fraction of $i$, and $M_i$ is the molar mass of $i$. Further assuming the system is spherical in nature and the density, $\varrho$, is known, the radius can be calculated as $R = \sqrt[3]{3m/4\pi\varrho}$.

### 2.1 The Poisson Distribution

A Poisson distribution can be obtained by considering a system with which there are zero (0) initial neutrons, there are no neutron interactions (no capture nor induced fission) such that $\lambda_c = \lambda_f = 0$, and there is a constant and randomly emitting singlet emitting neutron source, $S$, such that $q_\nu^S = \delta_{\nu,1}$. With these reductions, Eq. (1) becomes

$$\frac{\mathrm{d}P_n(t)}{\mathrm{d}t} = -SP_n(t) + SP_{n-1}(t), \tag{4}$$

with the initial condition $P_n(t=0) = \delta_{n,0}$. The solution to Eq. (4) is obtained by solving sequentially for $P_n(t)$ by starting at $n = 0$. In doing so, the solution can be deduced as:

$$P_n(t) = \frac{(St)^n}{n!}e^{-St}. \tag{5}$$

In the MC code, by setting $\sigma_f \equiv 0$ and $\sigma_c \approx 0$ (a very small number so that the MC simulation can calculate non-infinite interaction lengths; we used $\sigma_c = 10^{-300}\ cm^2$) we obtain a Poisson distribution of the neutron number, as seen in Fig. (1), where $S = 10.09799\ 1/sec$, $\alpha = -1.01229 \cdot 10^{-268}\ 1/sec$, $\tau = 9.87853 \cdot 10^{267}\ s$. As a matter of fact, since the source is singlet emitting and no induced fissions occur in this case, the cumulative fission PDF (which is only SF events) is exactly the neutron PDF. The results of Fig. (1) prove the MC simulation is sampling the source emission properly in time, we may now move on to incorporate neutron interactions with confidence.

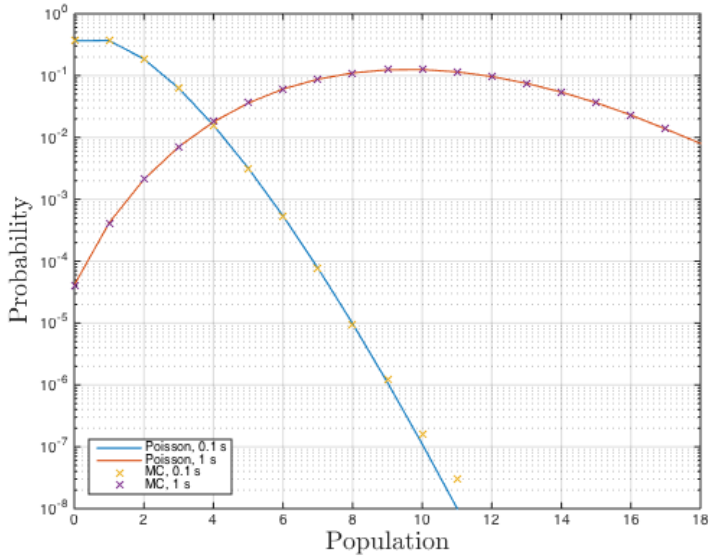


**Figure 1:** A comparison between a Poisson Distribution and Monte Carlo simulations for a system without fission or capture in the presence of a spontaneous fission source for two different final times.

### 2.2 The Binary Fission Model

For the binary fission model (BFM), we concern ourselves only with the possibility that two and only two neutrons are emitted per induced fission while one and only one neutron is emitted per source event; thus the respective multiplicity distributions of Eq. (1) become $q_\nu^f = \delta_{\nu,2}$ and $q_\nu^S = \delta_{\nu,1}$. With these restrictions on the fission multiplicity distributions, the master equation becomes

$$\frac{\mathrm{d}P_n(t)}{\mathrm{d}t} = -(\lambda_a n + S)P_n(t) + \lambda_c(n+1)P_{n+1}(t) + \Big[\lambda_f(n-1) + S\Big]P_{n-1}(t). \tag{6}$$

In order to derive an analytical distribution from Eq. (6), we employ the generating function

$$G(z,t) = \sum_{n=0}^{\infty} z^n P_n(t), \tag{7}$$

where $z \in [0,1]$ is real, to transform said equation into a partial differential equation of $G(z,t)$:

$$\frac{\partial G}{\partial t} = \left(\lambda_f z^2 - \lambda_a z + \lambda_c\right)\frac{\partial G}{\partial z} + S(z-1)G(z,t), \tag{8}$$

with an initial condition $G(z,0) = z^{n'}$, depending on how many neutrons, $n'$, are in the system at $t = 0$. Equation (8) can be solved with the method of characteristics, where we will now consider several special cases depending on the initial condition.

First, we simulate a system with zero initial neutrons so that $G(z,0) = 1$, with a spontaneous fission source. For this scenario, the solution to Eq. (8) can be determined with some work as

$$G(z,t) = \left[\frac{\alpha}{\alpha + \lambda_f b(t)}\right]^{\eta} \cdot \left[1 - \frac{\lambda_f b(t)}{\alpha + \lambda_f b(t)} z\right]^{-\eta}, \tag{9}$$

where $\eta = S/\lambda_f$ and

$$\begin{aligned} \alpha &= \lambda_f - \lambda_c = \frac{k-1}{\tau}, \\ b(t) &= e^{\alpha t} - 1. \end{aligned} \tag{10}$$

Here $k$ is the effective multiplication factor of the system and $\tau$ is the neutron lifetime. From here, to obtain the neutron number PDF, we expand the second bracketed term of Eq. (9) in a Taylor Series about $z = 0$ to find

$$G(z,t) = \left[\frac{\alpha}{\alpha + \lambda_f b(t)}\right]^{\eta} \cdot \sum_{n=0}^{\infty} \frac{\Gamma(\eta + n)}{n!\Gamma(\eta)} \left[\frac{\lambda_f b(t)}{\alpha + \lambda_f b(t)}\right]^n z^n, \tag{11}$$

and, by recalling the original definition of the generating function transform, Eq. (7), and comparing to Eq. (11) we can readily extract the solution to Eq. (6) as

$$P_n(t) = \left[\frac{\alpha}{\alpha + \lambda_f b(t)}\right]^{\eta} \cdot \left[\frac{\Gamma(\eta + n)}{n!\Gamma(\eta)}\right] \cdot \left[\frac{\lambda_f b(t)}{\alpha + \lambda_f b(t)}\right]^n, \tag{12}$$

where $\Gamma(z)$ is the gamma function. Note these expressions are valid for sub- and supercritical systems; in a subcritical system, $\alpha < 0$ and $b(t)$ decays with time, the opposite is true in a supercritical system. Figure (2) shows the comparison of Eq. (12) against the Monte Carlo for a subcritical stochastic system with a strong spontaneous fission source strength of $S = 5.048$ E6 $s^{-1}$, and some of the other system parameters are: $\sigma_f = 0.1$ $b$, $\sigma_c = 1.0$ $b$, $\alpha = -9.111$ E7 $s^{-1}$, and $\tau = 8.981 \cdot 10^{-9}$ $s$. These parameters provide a system multiplication factor of $k = \alpha\tau + 1 = 0.1817$, which is a highly subcritical system and, as one would expect, the probability of zero neutrons existing within the system at a given time dominates.

Next, we consider a system without a spontaneous fission source containing a single initial neutron such that the initial condition for the generating function is $G(z,0) = z$. The generating function PDE to solve is

$$\frac{\partial G(z,t)}{\partial t} = \left(\lambda_f z^2 - \lambda_a z + \lambda_c\right)\frac{\partial G}{\partial z}, \tag{13}$$

with an initial condition $G(z,0) = z$. From the Method of Characteristics, we see that the solution $G(z,t)$ is constant along it's characteristic curve (i.e., $\mathrm{d}G(z,t)/\,\mathrm{d}t = 0$) and we may set the solution equal to the initial condition $G(z,t) = G(z(t=0), t=0) = z(t=0)$. By solving the characteristic equation for $z$

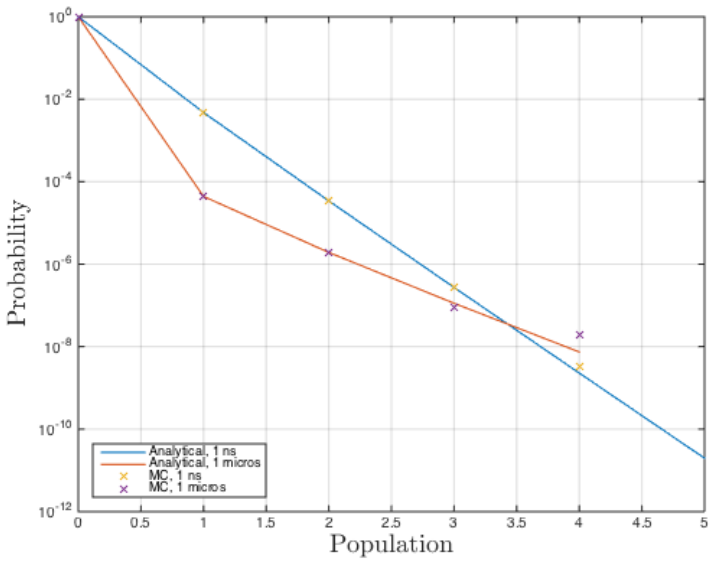


**Figure 2:** A comparison between Analytical and Monte Carlo simulations for a system with 0 initial neutrons in the presence of a spontaneous fission source at $t = 1ns$ and $t = 1\mu s$.

$$\frac{\mathrm{d}z}{\mathrm{d}t} = -\Big[\lambda_f z^2 - \lambda_a z + \lambda_c\Big], \tag{14}$$

with initial condition $z(t=0) = z_o$, we obtain the solution to Eq. (13), and Taylor expand about $z = 0$:

$$G(z,t) = \left[\frac{\lambda_c(1-e^{\alpha t})}{\lambda_c - \lambda_f e^{\alpha t}}\right] + \left[\frac{\alpha^2 e^{\alpha t}}{\lambda_f(\lambda_c - \lambda_f e^{\alpha t})(1-e^{\alpha t})}\right] \sum_{n=1}^{\infty} \left[\frac{\lambda_f(1-e^{\alpha t})}{\lambda_c - \lambda_f e^{\alpha t}}\right]^n z^n. \tag{15}$$

Comparing Eq. (15) to Eq. (7), we readily obtain the extinction probability and all higher $n$ probabilities as

$$P_0(t) = \frac{\lambda_c(1-e^{\alpha t})}{\lambda_c - \lambda_f e^{\alpha t}}, \tag{16a}$$

$$P_n(t) = \alpha^2 e^{\alpha t}\Big[\lambda_f(1-e^{\alpha t})\Big]^{n-1}\Big[\lambda_c - \lambda_f e^{\alpha t}\Big]^{-(n+1)}, \qquad n = 1,2,3,\ldots \tag{16b}$$

where we have simplified the $P_n(t)$ to avoid singularities when $\lambda_f = 0$ and/or when $t = 0$. Further analyzing Eqs. (16) when $t = 0$, we see that $P_0(0) = 0$, $P_1(0) = 1$ (by the identity $0^0 = 1$), and all $P_n(0) = 0$ for $n > 1$. Another extreme case to consider is that of a non-fissile system without a SF source and a single initiating neutron, for which we expect the PDF to be binary (i.e., only the extinction probability $P_0(t)$ and the singular probability $P_1(t)$ take on non-zero values). This can be shown to be true by setting $\lambda_f = 0$ in Eqs. (16) to find

$$P_0(t)|_{\lambda_f=0} = 1 - e^{-\lambda_c t},$$

$$P_n(t)|_{\lambda_f=0} = \lambda_c^{1-n} e^{-\lambda_c t}\Big[0(1-e^{-\lambda_c t})\Big]^{n-1}, \qquad n = 1,2,3,\ldots$$

We see that $P_1(t) = e^{-\lambda_c t}$ while all other $n > 1$ equal 0. Then $P_0(t)|_{\lambda_f=0} + P_1(t)|_{\lambda_f=0} = 1$, and the limiting value is $P_0(t)|_{\lambda_f=0} = 1$ as $t \to \infty$, suggesting definitive extinction for such a non-multiplying system. Using similar arguments for a multiplying supercritical system, we see that $P_n(\infty) = 0$, $P_0(\infty) = \lambda_c/\lambda_f$; thus, we find that the remainder of the probability is contained in the divergence probability $P_\infty(\infty) = 1 - \lambda_c/\lambda_f$.

It has been shown that the cumulative fission number PDF can be obtained for a lumped system for the special case of $\sigma_c = 0$ $b$, the PDF for such a system is

$$P_f(t) = e^{-t/\tau}\left[1 - e^{-t/\tau}\right]^f. \tag{17}$$

Figure (3) shows a comparison between the MC simulations and Eqs. (16) for the same system as before, but with no source and an initial neutron; Figure (4) is for the same system with no capture, for which Eq. (17) is valid.

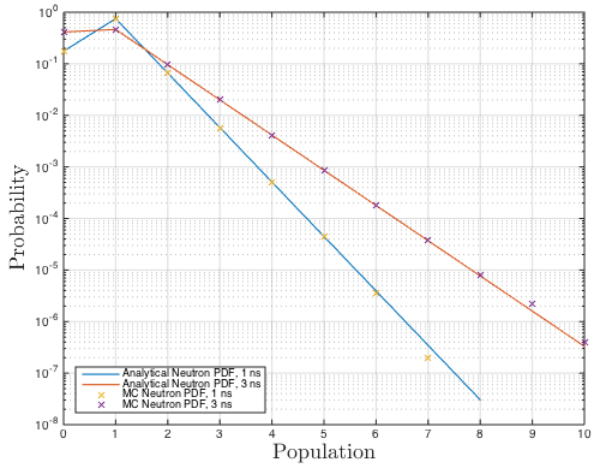


**Figure 3:** A comparison between Analytical and Monte Carlo simulations for a system with 1 initial neutron without a spontaneous fission source.

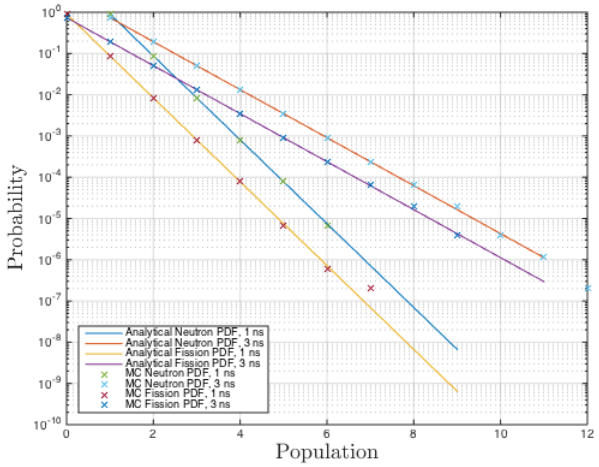


**Figure 4:** A comparison between Analytical and Monte Carlo simulations for a system with 1 initial neutron without a spontaneous fission source and no capture interactions.

Finally, the fission number distribution at $t = \infty$ for a supercritical system ($k_{eff} > 1$) consists of two components - a finite component corresponding to the cumulative number of fissions before the neutron number diverges, and an infinite component corresponding to the diverged neutron number which occurs with probability equal to the POI, the probabiltiy of initiation. The finite part of the distribution is given by

$$P_{F=0}(\infty) = 1 - p_f, \tag{18a}$$
$$P_F(\infty) = C_F p_f^F (1 - p_f)^{F+1}, \tag{18b}$$

where $C_F$ are the Catalan numbers defined as $C_F = (2F)!/[F!(F+1)!]$. Figure (5) shows a comparison between Eqs. (18) and the MC simulations.

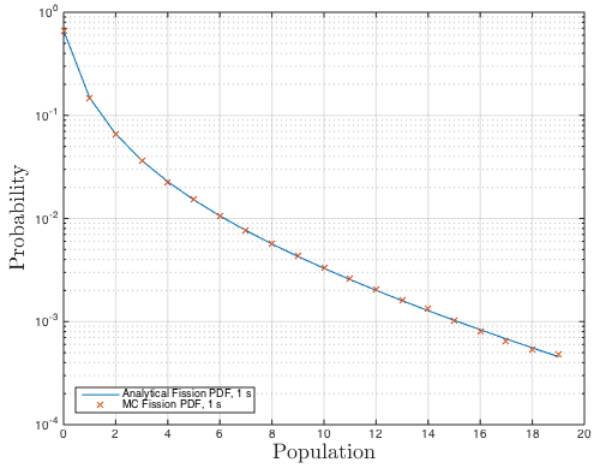


**Figure 5:** A comparison of the cumulative fission numbers calculated from Analytical and Monte Carlo simulations for a system in steady-state with 1 initial neutron without a spontaneous fission source.

### 2.3 Other Multiplicity Models to Consider

We now describe a numerical method for solving the steady-state Master equation for several multiplicity distribution models corresponding to a system composed of 20 $wt\%$ $^{240}Pu$ and 80 $wt\%$ $^{239}Pu$ [6] for which $\nu_m^f = 8$ and $\nu_m^S = 6$. We consider steady state only, in which case the Master equation for the equilibrium distribution for the BFM and general multiplicity case reduces to:

$$0 = -(n + S\tau)P_n + p_l(n+1)P_{n+1} + \Big[p_f(n-1) + S\tau\Big]P_{n-1}, \tag{19a}$$

$$0 = -(n + S\tau)P_n + p_l(n+1)P_{n+1} + S\tau\sum_{\nu=0}^{\nu_m^S} q_\nu^S P_{n-\nu}(t) + p_f\sum_{\nu=0}^{\nu_m} q_\nu^f(n-\nu+1)P_{n-\nu+1}, \tag{19b}$$

for $n = 0, 1, 2, \ldots$. As this is an open set of difference equations, it is necessary to truncate the neutron population at some finite number $N$ in order to obtain a numerical solution. For a subcritical system, this is feasible as the neutron number distribution decays with increasing order and can be assumed to vanish at an appropriately large $N$. Under this restriction, the population balance equations can be solved by writing Eqs. (19) as a recurrence relationship starting at $n = 0$. The first equation is not closed, but noting that the system of equations is linear and homogeneous, we initially set $P_0 = 1$, solve for the higher order $P_n$ successively from Eqs. (19) by forward recurrence until the number distribution has decayed to a sufficiently small value, and then obtain the true $P_0$ by enforcing normalization of the distribution.

Several multiplicity models can easily be investigated by changing the IF and/or SF multiplicity distributions, $q_\nu^{S/f}$; we consider three in particular, namely, the already well-defined BFM, the Full IF-Singlet Source emitting (FISS) model, and the Full IF-Full Source emission (FIFS) model. Ultimately, the FIFS is the model to compare any approximations to as it accounts for the entire neutron number emission spectrum for the given multiplicity distributions.

As stated before, we may rewrite Eqs. (19) in a forward recursion, thus, as an example for the FISS model, we are able to determine $P_{n+1}$ as a function of all lower $P_n$ probabilities by restricting $q_\nu^S = \delta_{\nu,1}$ to obtain the formula:

$$P_{n+1} = -\frac{1}{(p_f q_0^f + p_l)(n+1)} \Bigg\{ \Big[ (p_f q_1^f - 1)n - S\tau \Big] P_n + \Big[ p_f q_2^f (n-1) + S\tau \Big] P_{n-1} + p_f \sum_{\nu=3}^{8} q_\nu^f (n-\nu+1) P_{n-\nu+1} \Bigg\}. \tag{20}$$

Once the $N$ number probabilities have been calculated, we enforce the normalization condition to determine the actual extinction probability $P_0$ as:

$$P_0 = \left( 1 + \sum_{n=1}^{N} P_n \right)^{-1}. \tag{21}$$

From Eq. (21), the true PDF is determined by folding $P_0$ into all $P_n$ for $n > 0$. The forward recurrence is stable and the method is computationally efficient, allowing the computation of number distributions of very high order.

| $\Sigma_s$ | $\Sigma_f$ | $\Sigma_a$ | $\Sigma_t$ |
|---|---|---|---|
| 0.47488 | 0.20681 | 0.2766 | 0.9583 |

**Table 2:** Macroscopic Cross Sections

## 3 One-Dimensional Time Dependent Slab with Monoenergetic Neutrons

For a 1.0 $cm$ thick slab composed of pure $^{235}U$ metal with a density of $\rho = 19.1\ g/cm^3$, the $k_{eff} = 0.5686$, the neutron lifetime is $\tau = 1.0748\ sh$, which provides $\alpha = -0.4014\ sh^{-1}$. Several arbitrary final times and source strengths were chosen to compare the one-dimensional time-dependent monoenergetic Monte Carlo code to PARTISN's neutron population moments and cumulative induced fission moments calculator, see Appendix for details. The neutrons being modelled are monoenergetic with a constant velocity of $v = 1.0473\ cm/sh$. Using PARTISN's output file on such a system, the macroscopic cross sections in Table (2) were used and, to match with the MC, the MC microscopic cross sections were obtained by dividing these values by the number density: $\sigma_x = \Sigma_x/N$.

The process of time emission is the same as in the previous section regarding the lumped model MC, with the addition that the MC code was outfitted to allow for SF time-of-emission to be evenly distributed in time whereas the previous section sampled event times as exponentially decaying according to the Universal Law of Radioactive Decay. Further, we assume the source is evenly distributed in space and we can sample a SF event location $x$ by generating a random number $\xi$ such that $\xi \in [0, 1]$ using the equation

$$x = (x_R - x_L)\xi + x_L, \tag{22}$$

where $x_L$ and $x_R$ are the left and right boundary coordinates of the slab. From this source event, we sample the cosine of the angle of emission relative to the $x$-axis, $\mu$ such that $\mu \in [-1, 1]$, by assuming isotropic emission and, upon generating a new random number $\xi$, we have

$$\mu = 2\xi - 1. \tag{23}$$

Note that PARTISN considers singlet particle emission per event, but the MC code has been outfitted to allow for either singlet emitting or full multiplicity emission depending on the input data.

Now that we have a position of emission and a direction of travel, we must determine the distance travelled to the next collision site, $s$. The probability of a neutron travelling a distance $x'$ in the material without undergoing a collision is $\exp(-\Sigma_t x')$, while the probability of the same neutron travelling a short distance $\mathrm{d}x'$ and colliding is $\Sigma_t\,\mathrm{d}x'$. Thus, the appropriate cumulative distribution function for the probability of colliding a distance $s$, $F(s)$, to sample from is

$$F(s) = \xi = \int_0^s \Sigma_t e^{-\Sigma_t x'}\,\mathrm{d}x' \rightarrow s = -\frac{\ln(\xi)}{\Sigma_t}, \tag{24}$$

which provides the distance to the next collision site. The updated position within the slab, $x'$, relative to the $x$-axis is then calculated as $x' = x + s\mu$ and the updated time $t'$ is $t' = t + s/v$. We must now concern ourselves with four possible scenarios before we proceed:

1. $t' > t_f$, $x' \in [x_L, x_R]$: $n^0$ collision site is within the system and the $n^0$ is still in transit at $t_f$, bin as persistent $n^0$ and move onto the next particle.
2. $t' < t_f$, $x' \notin [x_L, x_R]$: $n^0$ collision site is out of the system and the $n^0$ arrives at site before $t_f$, bin as either left- or right-leaked $n^0$ and move onto the next particle.
3. $t' > t_f$, $x' \notin [x_L, x_R]$: $n^0$ has either leaked or persisted, we must determine the distance to the boundary and the time to get to the boundary and compare to the final time. Discussed below.
4. $t' < t_f$, $x' \in [x_L, x_R]$: $n^0$ collision site is within the system and the $n^0$ arrives at site before $t_f$, we continue on to sample which collision takes place. Discussed below.

| | Set of Histories | Set of Batches |
|---|---|---|
| Mean | $\mu = \frac{1}{h}\sum_{i=1}^{h} x_i$ | $\overline{x} = \frac{1}{B}\sum_{i=1}^{B} x_i$ |
| Variance | $\frac{1}{h}\sum_{i=1}^{h}(x_i-\mu)^2$ | $\frac{1}{B-1}\sum_{i=1}^{B}(x_i-\overline{x})^2$ |
| Skewness | $\sqrt{h}\frac{\sum_{i=1}^{h}(x_i-\mu)^3}{\left[\sum_{i=1}^{h}(x_i-\mu)^2\right]^{3/2}}$ | $\frac{B\sqrt{B-1}}{B-2}\frac{\sum_{i=1}^{B}(x_i-\overline{x})^3}{\left[\sum_{i=1}^{B}(x_i-\overline{x})^2\right]^{3/2}}$ |
| Kurtosis | $h\frac{\sum_{i=1}^{h}(x_i-\mu)^4}{\left[\sum_{i=1}^{h}(x_i-\mu)^2\right]^{2}}$ | $\frac{B(B+1)(B-1)}{(B-2)(B-3)}\frac{\sum_{i=1}^{B}(x_i-\overline{x})^4}{\left[\sum_{i=1}^{B}(x_i-\overline{x})^2\right]^{2}}$ |

**Table 3:** Equations for the moments for an individual batch and for the total set of batched simulations.

Concerning item 3, the collision site is out of the system and the time to get there is greater than the final time. To determine if the neutron is classified as persistent or leaked, we calculate the distance to the boundary, $s_b$, as

$$s_b = \begin{cases} s-(x-x_R)/\mu & \text{for } \mu > 0 \\ s-(x-x_L)/\mu & \text{for } \mu < 0. \end{cases} \tag{25}$$

Recall $x$ is the original location of the neutron, not the collision site. We then determine the time to get to the boundary, $t_b$, as being

$$t_b = t + \frac{s_b}{v}, \tag{26}$$

where $t$ is, again, the time that the neutron was at the original site. We can then determine whether the neutron was in the system at the final time, if $t_b > t_f$ (the time to get to the boundary was greater than the final time), or if it had leaked, $t_b < t_f$.

Concerning item 4, we must then proceed to sample from the discrete CDF of the microscopic cross-sections, which is similar to the lumped CDF but with the inclusion of scattering. Thus, a random number $\xi$ is chosen and first compared to the ratio $\sigma_c/\sigma_t$ and if $\xi < \sigma_c/\sigma_t$, the neutron is captured and we proceed to the next particle. If $\sigma_c/\sigma_t \leq \xi < (\sigma_c+\sigma_s)/\sigma_t$, we scatter the neutron and repeat the process starting at Eq. (23). Finally, if $\xi \geq (\sigma_c+\sigma_s)/\sigma_t$, the neutron has induced a fission and we proceed to follow the chain of particles until it has persisted past $t_f$, has diverged to a population greater than a prescribed limit, or has died away.

The moments of the neutron number and cumulative induced fission number distributions were calculated by partitioning a total set of simulations into batches, determining the first four moments for each batch to construct a sample distribution of calculated moments, and finally deriving the reported results from the moments of the distributions of the batch moments. To explain this in more detail, a batch may contain several thousands or even millions of simulations (a.k.a. histories) with unique independent identically distributed (IID) outcomes. For a single batch, the mean, variance, skewness, and kurtosis are calculated using the equations in the "Set of Histories" column of Table (3) and saved for post-processing, where $h$ is the number of histories performed per batch. Once all of the batches are completed, a distribution of the batch moments is obtained and is expected to approach the Gaussian distribution in accordance with the Law of Large Numbers for IID random variables. It can be seen in Table (4) that the skewness is near zero, indicating a symmetric distribution about the mean, and the kurtosis hovers around three as does the Gaussian distribution. From this normal distribution, we use the equations in the "Set of Batches" column of Table (3) to find the moments of the entire set of histories for a total number of $B$ batches. Note that the minimal number of batches is four to avoid a singularity from the coefficient of the batch kurtosis.

Tables (5) and (6) summarize the moments of the neutron number PDF as well as the cumulative induced fission number PDF as calculated by PARTISN and the MC code for several scenarios for the previously mentioned slab

| Batches | Histories/Batch | $S$, $[cm^{-3}s^{-1}]$ | $t_f$, $[s]$ | $s_{\overline{N}}$ | $\kappa_{\overline{N}}$ | $s_{\overline{F}}$ | $\kappa_{\overline{F}}$ |
|---|---|---|---|---|---|---|---|
| 100 | 4 E7 | 25,057.4 | 5.69 E-6 | 0.117 | 2.89 | 0.488 | 3.47 |
| 500 | 4 E7 | 100,000 | 1.0 E-5 | -3.46 E-2 | 3.14 | 7.12 E-2 | 2.82 |
| 500 | 4 E7 | 10.0 | 1.0 E-3 | -0.145 | 2.87 | -2.58 E-2 | 3.02 |
| 50 | 1 E6 | 2,249.014 | 2.851 E-3 | -0.186 | 3.14 | 0.159 | 2.96 |
| 500 | 4 E7 | 0.154 | 1.1 E-2 | -1.1 E-2 | 3.11 | 5.63 E-2 | 2.76 |

**Table 4:** Skewness and kurtosis for the mean neutron number $\overline{N}$ and the mean cumulative fission number $\overline{F}$ for several sources and final times for a slab of $L = 1$ $cm$ with monoenergetic neutrons.

arrangement. The highlighted calculated percent error is relative to the PARTISN values and the median MC value and is already displayed as a percentage. The large difference between the percentage errors for the neutron numbers of Table (5) and the cumulative induced fission numbers of Table (6) for corresponding source strengths and final times is most likely attributed to the low number of total fissions to occur for each individual history and, thus, we obtain poorer statistical certainty on the PDF for these outcomes. For such systems with low cumulative fission numbers where the fission PDF is dominated by the extinction probability, or rather the non-existence probability, the required number of histories per batch is inversely proportional to the smallest probability one desires to obtain. This makes the storage cumbersome when more than $10^7$ histories per batch are required as an array of that size is required to store the data for each counter (for both the neutron number and the fission number, as well as any other moments one might be calculating, such as leaked neutron PDFs).

The confidence interval, $C_j$, for the $j^{th}$ moment was calculated using the 95% confidence coefficient of 1.96 multiplied by the sample distribution standard deviation as:

$$C_j = 1.96\frac{\sigma_j}{\sqrt{B}}, \tag{27}$$

where $B$ is the total number of batches. These values are reported directly after the median values of the MC simulation and show that the majority of the PARTISN results fall within the 1.96 standard deviations or are very close to either the upper or lower bounds.

Also of interest are the actual probability distribution functions of the neutron number and cumulative induced fission number for which the moments of have been the focus in this section. The Monte Carlo code has the capability to reproduce the PDFs by constructing a histogram with size and bin widths based on the greatest valued outcome from the first batch of histories. After the first batch, a subroutine is called and builds the necessary histograms and corresponding grids with the bin mesh points. If any histories have an outcome greater than the greatest of the first batch, they are placed into the last bin. The PDFs for the neutron number at a final time are surmised in Figure 6(a) and the cumulative induced fission number within the time interval are shown in Figure 6(b).

| Code | Histories | $S$, $[cm^{-3}s^{-1}]$ | $t_f$, $[s]$ | $\overline{N}$ | $\sigma_N$ | $s_N$ | $\kappa_N$ |
|---|---|---|---|---|---|---|---|
| PARTISN | - | 25,057.4 | 5.69 E-5 | 1.4258 | 1.1941 | 8.3756 E-1 | 3.7017 |
| MC | 4 E9 | 25,057.4 | 5.69 E-5 | 1.4258 ± 4.1E-5 | 1.1941 ± 3.1E-5 | 8.3751 E-1 ± 9.8E-5 | 3.7014 ± 4.5E-4 |
| % Error | - | - | - | 0.00000 | 0.00000 | 0.00597 | 0.00811 |
| PARTISN | - | 100,000 | 1.0 E-5 | 1.0000 | 1.0000 | 1.0000 | 4.0001 |
| MC | 2 E10 | 100,000 | 1.0 E-5 | 1.0000 ± 1.4E-5 | 1.0000 ± 1.1E-5 | 1.0000 ± 4.3E-5 | 4.0001 ± 2.3E-4 |
| % Error | - | - | - | 0.00000 | 0.00000 | 0.00000 | 0.00000 |
| PARTISN | - | 10.0 | 1.0 E-3 | 9.9976 E-3 | 1.0002 E-1 | 10.016 | 103.8 |
| MC | 2 E10 | 10.0 | 1.0 E-3 | 9.9963 E-3 ± 1.4E-6 | 9.9998 E-2 ± 7.2E-6 | 10.011 ± 8.2E-4 | 103.5 ± 2.4E-2 |
| % Error | - | - | - | 0.0130 | 0.0220 | 0.0499 | 0.2890 |
| PARTISN | - | 2,249.014 | 2.851 E-3 | 6.4087 | 2.5335 | 3.9676 E-1 | 3.1597 |
| MC | 5 E7 | 2,249.014 | 2.851 E-3 | 6.4076 ± 2.3E-3 | 2.5330 ± 1.8E-3 | 3.9598 E-1 ± 2.3E-3 | 3.1557 ± 6.8E-3 |
| % Error | - | - | - | -0.07552 | 0.3927 | -0.6931 | -0.3982 |
| PARTISN | - | 0.154 | 1.1 E-2 | 1.6912 E-3 | 4.1244 E-2 | 24.733 | 647.1 |
| MC | 2 E10 | 0.154 | 1.1 E-2 | 1.6894 E-3 ± 5.8E-7 | 4.1174 E-2 ± 7.2E-6 | 24.579 ± 6.7E-3 | 626.2 ± 0.8 |
| % Error | - | - | - | 0.1064 | 0.1697 | 0.6226 | 3.2297 |

**Table 5:** Neutron population results for several different source strengths and different final times for a slab of $L = 1\ cm$ with monoenergetic neutrons.

| Code | Histories | $S$, $[cm^{-3}s^{-1}]$ | $t_f$, $[s]$ | $\overline{F}$ | $\sigma_F$ | $s_F$ | $\kappa_F$ |
|---|---|---|---|---|---|---|---|
| PARTISN | - | 25,057.4 | 5.69 E-5 | 8.7852 E-6 | 2.9640 E-3 | 3.3739 E2 | 1.1384 E5 |
| MC | 4 E9 | 25,057.4 | 5.69 E-5 | 8.7797 E-6 ± 1.1E-7 | 2.9614 E-3 ± 1.9E-5 | 3.3802 E2 ± 2.2 | 1.1438 E5 ± 1.5E3 |
| % Error | - | - | - | 0.0626 | 0.0877 | -0.1867 | -0.4743 |
| PARTISN | - | 100,000 | 1.0 E-5 | 1.0829 E-6 | 1.0406 E-3 | 960.96 | 9.2346 E5 |
| MC | 2 E10 | 100,000 | 1.0 E-5 | 1.0676 E-6 ± 1.5E-8 | 1.0301 E-3 ± 7.1E-6 | 977.02 ± 6.9 | 9.6083 E5 ± 1.4E4 |
| % Error | - | - | - | 1.4129 | 1.0090 | -1.6712 | -4.0467 |
| PARTISN | - | 10.0 | 1.0 E-3 | 1.0827 E-6 | 1.0407 E-3 | 961.52 | 9.2518 E5 |
| MC | 2 E10 | 10.0 | 1.0 E-3 | 1.0823 E-6 ± 1.4E-8 | 1.0375 E-3 ± 6.8E-6 | 969.57 ± 6.6 | 9.4582 E5 ± 1.3E4 |
| % Error | - | - | - | 0.0369 | 0.3075 | -0.8372 | -2.2309 |
| PARTISN | - | 2,249.014 | 2.851 E-3 | 1.9790 E-3 | 4.4509 E-2 | 22.5127 | 510.8 |
| MC | 5 E7 | 2,249.014 | 2.851 E-3 | 1.9688 E-3 ± 4.4E-5 | 4.4355 E-2 ± 5.0E-4 | 22.6176 ± 0.26 | 516.1 ± 12.0 |
| % Error | - | - | - | -0.3527 | -0.1267 | 0.3220 | 0.8332 |
| PARTISN | - | 0.154 | 1.1 E-2 | 2.0157 E-6 | 1.4225 E-3 | 708.44 | 5.0574 E5 |
| MC | 2 E10 | 0.154 | 1.1 E-2 | 2.0166 E-6 ± 1.9E-8 | 1.4201 E-3 ± 6.8E-6 | 710.41 ± 3.5 | 5.0897 E5 ± 5.2E3 |
| % Error | - | - | - | 0.0446 | 0.1687 | -0.2781 | -0.6387 |

**Table 6:** Cumulative induced fission number results for several different source strengths and different final times for a slab of $L = 1$ $cm$ with monoenergetic neutrons.

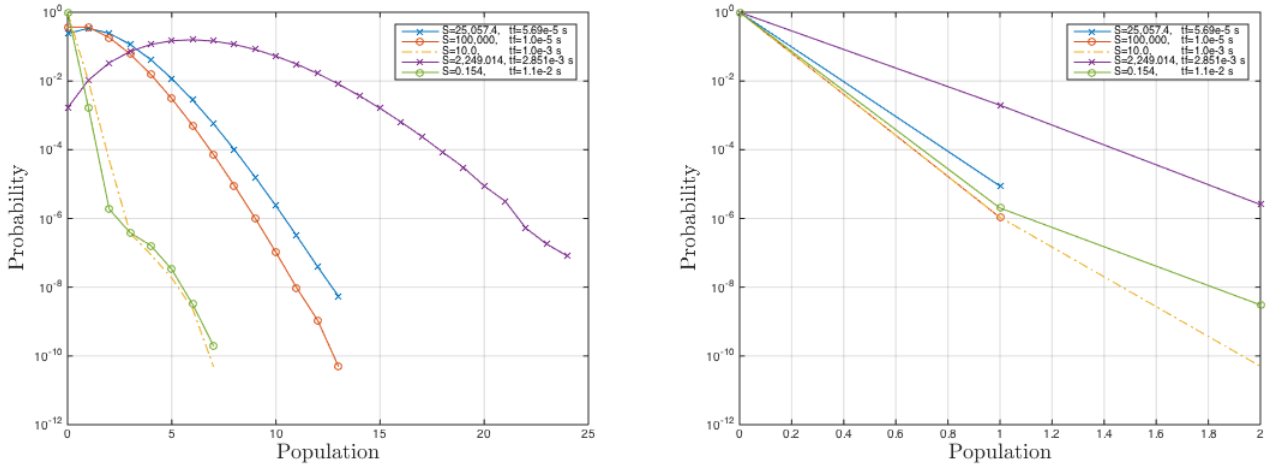


**((a))** Neutron number. **((b))** Cumulative induced fission number.

**Figure 6:** PDFs for the neutron number and the cumulative induced fission number for a given final time and source strength ($S$ has units of $cm^{-3}s^{-1}$).

## 4 A Time Dependent Sphere with Monoenergetic Neutrons

The next stage in the development of the MC code is to convert from a one-dimensional slab into a one-dimensional sphere with monoenergetic neutrons. We maintain the assumptions that source emission as well as scattering events are isotropic and that the source is evenly distributed in space. In order to sample locations of spontaneous fission events within our sphere, the spatial probability density function at a radial position, $f(r)$, must depend on the mass associated with that position. The mass of a sphere is proportional to the volume $V$ and and incremental mass is proportional to the volume of an incremental shell, $\mathrm{d}V$, and we can say the appropriate spatial probability distribution is [5]

$$f(r)\,\mathrm{d}r = \frac{\mathrm{d}V}{V} = \frac{3r^2}{R^3}\,\mathrm{d}r, \tag{28}$$

and the cumulative distribution function $F(r)$ for which to sample a radial position of emission is then

$$F(r) = \xi = \int_0^r f(r')\,\mathrm{d}r' \quad \rightarrow \quad r = \xi^{1/3}R, \tag{29}$$

where $R$ is the radius of the system, $r \leq R$, and per usual, $\xi \in [0,1]$ is a randomly generated number. Once the radial position is known, we sample an angle of emission, assumed to be isotropic, and use Eq. (23). Note that $\mu \in [-1,1]$ is now the cosine of the angle made between the radial coordinate vector and the direction of neutron travel, which is different from some prescribed Cartesian axis. Next, the distance to collision is sampled using Eq. (24) and the new radial position $r'$ is updated using

$$r' = \sqrt{r^2 + s^2 + 2rs\mu}, \tag{30}$$

and the updated time of collision $t'$ is $t' = t + s/v$. We use the same logical outline that is enumerated in the previous section to determine the next operation to perform on the neutron with the new exception that we only need to compare $r'$ to the system radius $R$. Thus, if $t' > t_f$ and $r' < R$, the neutron is a persistent neutron and move onto the next particle; if $t' < t_f$ and $r' > R$, the neutron has leaked; if $t' < t_f$ and $r' < R$, we sample which interaction occurs just as before; and if $t' > t_f$ and $r' > R$, we must determine whether the neutron was still in the system or outside the system at $t_f$. For this last case, we calculate the distance to the boundary $s_b$ using

$$s_b = \sqrt{R^2 - r^2(1-\mu^2)} - r\mu. \tag{31}$$

| Batches | Histories/Batch | $S$, $[cm^{-3}s^{-1}]$ | $t_f$, $[s]$ | $s_{\overline{N}}$ | $\kappa_{\overline{N}}$ | $s_{\overline{F}}$ | $\kappa_{\overline{F}}$ |
|---|---|---|---|---|---|---|---|
| 50 | 1 E7 | 25,057.4 | 5.69 E-5 | 0.209 | 2.344 | -0.470 | 3.897 |
| 50 | 1 E7 | 100,000 | 1.0 E-5 | 0.316 | 3.48 | 0.231 | 3.083 |
| 50 | 1 E7 | 10.0 | 1.0 E-3 | -5.765 E-2 | 3.106 | 0.275 | 3.224 |
| 1 E3 | 1 E3 | 2,249.014 | 2.851 E-3 | -4.109 E-2 | 3.017 | 0.103 | 3.009 |
| 1 E3 | 1 E6 | 0.154 | 1.1 E-2 | -4.609 E-2 | 3.034 | 0.156 | 2.759 |

**Table 7:** Skewness and kurtosis for the mean neutron number $\overline{N}$ and the mean cumulative fission number $\overline{F}$ for several sources and final times for a sphere of $R = 2\ cm$ with monoenergetic neutrons.

From which, the time at which the neutron intersects the spherical surface, $t_b$, is calculated using Eq. (26) which will inform us whether the neutron had leaked or was still in the system at the final time.

Once again, this process is carried out many times in order to gain the desired level of confidence in the final calculated tallies. The batching statistics method has been employed, as described in the previous section, and the third and fourth moments of the batched distributions for the mean number of neutrons at $t_f$ and the mean cumulative number of induced fissions is shown in Table 7.

| Code | Histories | $S$, $[cm^{-3}s^{-1}]$ | $t_f$, $[s]$ | $\overline{N}$ | $\sigma_N$ | $s_N$ | $\kappa_N$ |
|---|---|---|---|---|---|---|---|
| PARTISN | - | 25,057.4 | 5.69 E-5 | 47.7779 | 6.9123 | 0.1447 | 3.0209 |
| MC | 5 E8 | 25,057.4 | 5.69 E-5 | 47.7781 ± 6.0E-4 | 6.9124 ± 4.2E-4 | 0.1446 ± 2.3E-4 | 3.0207 ± 5.3E-4 |
| % Error | - | - | - | -0.0004 | -0.0014 | 0.0691 | 0.0066 |
| PARTISN | - | 100,000 | 1.0 E-5 | 33.5103 | 5.7888 | 0.1728 | 3.0298 |
| MC | 5 E8 | 100,000 | 1.0 E-5 | 33.5106 ± 4.6E-4 | 5.7890 ± 4.2E-4 | 0.1729 ± 2.4E-4 | 3.0298 ± 5.0E-4 |
| % Error | - | - | - | -0.0009 | -0.0035 | -0.0579 | 0.0000 |
| PARTISN | - | 10.0 | 1.0 E-3 | 0.3350 | 0.5790 | 1.7303 | 6.0087 |
| MC | 5 E8 | 10.0 | 1.0 E-3 | 0.3351 ± 3.7E-5 | 0.5789 ± 4.1E-5 | 1.7292 ± 3.0E-4 | 5.9988 ± 2.2E-3 |
| % Error | - | - | - | -0.0299 | 0.0000 | 0.0694 | 0.1731 |
| PARTISN | - | 2,249.014 | 2.851 E-3 | 214.797 | 14.6676 | 6.8533 E-2 | 3.0048 |
| MC | 1 E6 | 2,249.014 | 2.851 E-3 | 214.859 ± 2.7E-2 | 14.6416 ± 1.9E-2 | 6.8119 ± 5.0E-3 | 2.9975 ± 9.8E-3 |
| % Error | - | - | - | -0.0288 | 0.1773 | 0.6041 | 0.2429 |
| PARTISN | - | 0.154 | 1.1 E-2 | 5.6664 E-2 | 0.2388 | 4.2710 | 22.2053 |
| MC | 1 E9 | 0.154 | 1.1 E-2 | 5.6734 ± 1.5E-5 | 0.2386 ± 3.4E-5 | 4.2419 ± 1.1E-3 | 21.5781 ± 2.3E-2 |
| % Error | - | - | - | -0.1235 | 0.0838 | 0.6813 | 2.8246 |

**Table 8:** Neutron population results for several different source strengths and different final times for a sphere of $R = 2$ $cm$ with monoenergetic neutrons.

| Code | Histories | $S$, $[cm^{-3}s^{-1}]$ | $t_f$, $[s]$ | $\overline{F}$ | $\sigma_F$ | $s_F$ | $\kappa_F$ |
|---|---|---|---|---|---|---|---|
| PARTISN | - | 25,057.4 | 5.69 E-5 | 2.9440 E-4 | 1.7158 E-2 | 58.2837 | 3.4001 E3 |
| MC | 5 E8 | 25,057.4 | 5.69 E-5 | 2.9468 E-4 ± 1.6E-6 | 1.7166 E-2 ± 4.6E-5 | 58.2687 ± 0.16 | 3.3991 E3 ± 19.2 |
| % Error | - | - | - | -0.0951 | -0.0466 | 0.0257 | 0.0294 |
| PARTISN | - | 100,000 | 1.0 E-5 | 3.6289 E-5 | 6.0240 E-3 | 166.00 | 2.7560 E4 |
| MC | 5 E8 | 100,000 | 1.0 E-5 | 3.6282 E-5 ± 6.1E-7 | 6.0209 E-3 ± 5.1E-5 | 166.25 ± 1.4 | 2.7672 E4 ± 460.4 |
| % Error | - | - | - | 0.01929 | 0.0515 | -0.1506 | -0.4064 |
| PARTISN | - | 10.0 | 1.0 E-3 | 3.6285 E-5 | 6.0249 E-3 | 166.10 | 2.7611 E4 |
| MC | 5 E8 | 10.0 | 1.0 E-3 | 3.6112 E-5 ± 3.6E-7 | 5.9903 E-3 ± 3.0E-5 | 168.09 ± 0.86 | 2.8453 E4 ± 295 |
| % Error | - | - | - | -0.4437 | -0.1743 | -0.1987 | 0.4237 |
| PARTISN | - | 2,249.014 | 2.851 E-3 | 6.6326 E-2 | 0.2577 | 3.8888 | 18.1528 |
| MC | 1 E6 | 2,249.014 | 2.851 E-3 | 6.6294 E-2 ± 5.2E-4 | 0.2567 ± 1.1E-3 | 3.8764 ± 2.2E-2 | 17.8493 ± 2.4E-1 |
| % Error | - | - | - | 0.0482 | 0.3880 | 0.3189 | 1.6719 |
| PARTISN | - | 0.154 | 1.1 E-2 | 6.7582 E-5 | 8.2368 E-3 | 122.354 | 1.5089 E4 |
| MC | 1 E9 | 0.154 | 1.1 E-2 | 6.7370 E-5 ± 5.0E-7 | 8.2093 E-3 ± 3.1E-5 | 123.17 ± 0.47 | 1.5331 E4 ± 121.6 |
| % Error | - | - | - | 0.3137 | 0.3339 | -0.6669 | -1.6038 |

**Table 9:** Cumulative induced fission number results for several different source strengths and different final times for a sphere of $R = 2$ $cm$ with monoenergetic neutrons.

| | $\overline{N}$ | $\sigma_N$ | $s_N$ | $\kappa_N$ | $\overline{F}$ | $\sigma_F$ | $s_F$ | $\kappa_F$ |
|---|---|---|---|---|---|---|---|---|
| PARTISN | 0.3350 | 0.5790 | 1.7303 | 6.0087 | 3.6285 E-5 | 6.0249 E-3 | 166.10 | 2.7611 E4 |
| MEMC | 0.3351 | 0.5789 | 1.7292 | 5.9988 | 3.6112 E-5 | 5.9903 E-3 | 168.09 | 2.8453 E4 |
| % | -0.0299 | 0.0173 | 0.0694 | 0.1731 | -0.4437 | -0.1743 | -0.1987 | 0.4237 |
| MGMC | 0.3350 | 0.5789 | 1.7293 | 5.9996 | 3.6580E-5 | 6.0465E-3 | 165.66 | 2.7492 E4 |
| % | 0.0000 | 0.0173 | 0.0578 | 0.1514 | -0.8130 | -0.3585 | 0.2649 | 0.4310 |

**Table 10:** Comparison between PARTISN, the monoenergetic Monte Carlo (MEMC), and the multigroup one-group Monte Carlo for a spherical system (MGMC).

## 5 A Time Dependent Sphere with Multigroup Energy Binning

The final step in the development of the MC code for the summer project involves the incorporation of multigroup energy binning of the neutrons. This is pivotal in benchmarking PARTISN's moment calculators as it uses multigroup data to solve the adjoint transport equations of the respective moments that have been under investigation throughout this report. Extending the MC to account for multigroup neutrons is accomplished by converting the cross-sections, multiplicity distributions, and sources into arrays (with max dimension equal to the number of energy groups) that are then used to sample a neutron's energy, i.e. energy bin. As an example, if a neutron appears as a result of a spontaneous fission, the discrete cumulative distribution function of the group-dependent source strengths are sampled to determine the energy, whereas a neutron born from an induced fission will have it's energy sampled from the chi spectrum. The data is extracted from the PARTISN output file and this allows one to construct the necessary CDFs for energy bin sampling as a means of replicating the exact same system that the multigroup adjoint deterministic transport code is solving.

Perhaps the most important difference between the monoenergetic and the multigroup calculations is found in the scattering interactions. As it turns out, PARTISN has absorption-emission events, such as ($n$,2$n$), included/embedded in the scattering matrix produced in the output file. Thus, it has proven necessary to include these events in the simulation process by calculating an effective $\overline{\nu}_{g,S}$ for scattering events as a function of the incident neutron energy and sampling the number of neutrons created in every scatter event. This sampling is done by selecting a random number $\xi \in [0,1]$ and comparing it to the difference $d = \overline{\nu}_{g,S} - \lfloor \overline{\nu}_{g,S} \rfloor$, so that if $\xi \leq d$, the number of neutrons born in the scatter event is $\lceil \overline{\nu}_{g,S} \rceil$, and if $\xi > d$, the number of neutrons born in the scatter event is $\lfloor \overline{\nu}_{g,S} \rfloor$. Note that the notation $\lfloor a \rfloor$ and $\lceil a \rceil$ refers to the floor of $a$ (the next smallest integer) and the ceiling of $a$ (the next highest integer), respectively. Ideally it would be most desirable to sample the number of neutrons created in an ($n$,$xn$) reaction from a multiplicity distribution, just as with any other stochastic neutron source, rather than sampling only two possible outcomes about the average number emitted per scatter event.

The first test to ensure the code is performing correctly is to compare a one-group simulation of the multigroup code with that of the monoenergetic sphere and with PARTISN. Seen in Table (10), the one-group multigroup agrees with monoenergetic and PARTISN calculations for a sphere of radius $R = 2\ cm$, $S = 10.0\ cm^{-3}s^{-1}$ and $t_f = 1.0\ ms$. These results provide confidence in our ability to produce the same results as a one-group calculation upon collapsing to a single energy group.

We next consider the famous Lady Godiva critical assembly experiment with three energy groups with a slightly larger radius to simulate a supercritical system. With a radius of $R = 7.70\ cm$, a uniform density of $\rho = 18.74\ g/cc$, 20 ordinates, along with using mendf6 library and 93.71 $wt\%$ $^{235}U$ oralloy (Oak Ridge alloy), PARTISN calculates

| | $\overline{N}$ | $\sigma_N$ | $s_N$ | $\kappa_N$ | $\overline{F}$ | $\sigma_F$ | $s_F$ | $\kappa_F$ |
|---|---|---|---|---|---|---|---|---|
| PARTISN | 0.2685 | 0.5183 | 1.9329 | 6.7617 | 7.5834 E-6 | 2.7539 E-3 | 363.16 | 1.3191 E5 |
| MGMC | 0.2685 | 0.5183 | 1.9318 | 6.7497 | 7.6480 E-6 | 2.8161 E-3 | 355.90 | 1.2995 E5 |
| % Error | 0.0000 | 0.0000 | 0.0569 | 0.1775 | -0.8519 | -2.2586 | 1.9991 | 1.4859 |

**Table 11:** Lady Godiva results as simulated by PARTISN as well as the multigroup MC code.

| | $\overline{N}$ | $\sigma_N$ | $s_N$ | $\kappa_N$ | $\overline{F}$ | $\sigma_F$ | $s_F$ | $\kappa_F$ |
|---|---|---|---|---|---|---|---|---|
| PARTISN | 39.5616 | 6.5336 | 0.2092 | 3.0785 | 0.2002 | 0.4515 | 2.2957 | 8.4514 |
| MGMC | 39.1466 | 6.3886 | 0.2052 | 3.0374 | 0.2021 | 0.4507 | 2.2412 | 8.0537 |
| % Error | 1.0490 | 2.2193 | 1.9120 | 1.3351 | -0.9491 | 0.1772 | 2.3740 | 4.7057 |

**Table 12:** Jezebel results as simulated by PARTISN as well as the multigroup MC code.

$k = 1.0152345$ for $t_f = 3.120\ \mu s$. It is seen in Table (11) that we have excellent agreement between the two codes for the neutron number, but the cumulative induced fission number is showing as much as several percentage error. This difference can be attributed to the oscillatory nature of the results of the MC as a function of the number of histories and batches performed. If we were to increase the total number of histories towards infinity, we should see a convergence to the statistically true answer, which seems to be close to the values produced by PARTISN. This has yet to be tested in this report.

Finally, we consider a 12-group supercritical simulation of Jezebel with a radius of $R = 6.385\ cm$, a uniform density of $\rho = 15.61\ g/cc$, 20 ordinates, and using mendf6 library and 95.5 $at\%\ ^{239}Pu$, PARTISN calculates $k = 1.1267305$ for $t_f = 5.0\ sh$. Due to stringent time, the simulation could not be performed to produce optimally agreeable results, but it can be seen that for a quick calculation, the multigroup MC produces results very close to PARTISN's, which is very promising.

## 6 Conclusion

It has been shown that a spherical coordinate, multigroup, time-dependent, neutron transport analog Monte Carlo code designed to calculate the moments of the neutron number probability distribution as well as the cumulative induced fission probability distribution agrees well with LANL's deterministic transport code, PARTISN. This was done by continual benchmarking of the Monte Carlo code during the development from a strictly time-dependent code into the capstone version just mentioned. This agreement not only provides confidence that the Monte Carlo code can be extended to include multiregion geometries, include anisotropic neutron scattering, but also allows PARTISN to consider multiplet source emission and, more importantly, verifies the deterministic transport methods utilized by PARTISN.

# 7 Appendix

## 7.1 Neutron Moments Using Deterministic Transport

The moments of the neutron population have been derived [1] using equations of stochastic neutronics which were first formulated by Bell [7] and Pal [8]. The derivation requires us to first consider a single initial neutron and all the progeny resulting from its introduction into the system. Following Bell's derivation, one arrives at the probability of there existing $n$ neutrons in a region $R$ at a final time $t_f$ due to a neutron being born at $\vec{r}$ with velocity $\vec{v}$, at an earlier time $t < t_f$ is

$$P_n(R,t_f;\vec{r},\vec{v},t) = A + \int \mathrm{d}s\Sigma_t\Big(\vec{r}+s\hat{\Omega},\vec{v},t+\frac{s}{v}\Big)e^{-\int \mathrm{d}s'\Sigma_t\left(\vec{r}+s'\hat{\Omega},\vec{v},t+\frac{s'}{v}\right)} \times \Bigg[c_0\Big(\vec{r}+s\hat{\Omega},\vec{v},t+\frac{s}{v}\Big)\delta_{n,0} + \sum_{j=1}^{\nu_m}\int \mathrm{d}\vec{v}_1\cdots\int \mathrm{d}\vec{v}_j c_j\Big(\vec{r}+s\hat{\Omega},\vec{v}\to\{\vec{v}_1\ldots\vec{v}_j\},t+\frac{s}{v}\Big)\sum_{M_j=0}^{n}\prod_{i=1}^{j}P_{m_i}\Big(\vec{r}+s\hat{\Omega},\vec{v}_i,t+\frac{s}{v}\Big)\Bigg], \tag{32}$$

where $\Sigma_t$ is the macroscopic total cross-section, $c_j$ is the probability of $j$ neutrons being emitted in an induced fission, $v = |\vec{v}|$ is the speed of the incident neutron, $A$ is a correction factor that accounts for the possibility that the neutron did not interact either before leaking or before the final time, and $M_j = \sum_{k=1}^{j} m_k$ such that the $M_j$ take on all possible combinations of neutron chain numbers that add to $n$; each $m_k$ corresponds to a summation from 0 to $n$ such that it contributes to the current value of $M_j$. This non-linear system of fully-coupled equations cannot be solved directly without knowing the maximum number of neutrons in the system, $n_{max}$, for which an equation corresponds to each possible population number, which cannot be inferred in general and is frequently a very large number.

Thus, we introduce the probability density generating function (PDGF) transformation, $\mathcal{G}$, which condenses Eq. (32) from a set of $n_{max}$ equations into a single adjoint transport-like equation. The PDGF is defined as

$$\mathcal{G}(z;\vec{r},\vec{v},t) = 1 - \sum_{n=0}^{\infty} z^n P_n(R,t_f;\vec{r},\vec{v},t), \tag{33}$$

where we will neglect to write $\mathcal{G}$ to be a function of $R, t_f$ for brevity; also, $z$ is a real variable restricted to $z \in [0,1]$ to ensure convergence of the summation of Eq. (33). We then multiply Eq. (32) by $z^n$, sum over all $n$, and subtract from unity to obtain:

$$-\frac{1}{v}\frac{\partial\mathcal{G}}{\partial t} - \hat{\Omega}\cdot\nabla\mathcal{G} + \Sigma_t(\vec{r},\vec{v},t)\mathcal{G}(z;\vec{r},\vec{v},t) = \int \mathrm{d}\vec{v}'\Sigma_s(\vec{r},\vec{v}\to\vec{v}',t)\mathcal{G}(z;\vec{r},\vec{v}',t) + \overline{\nu}\Sigma_f(\vec{r},\vec{v},t)\int \mathrm{d}\vec{v}'\chi(\vec{v}\to\vec{v}')\mathcal{G}(z;\vec{r},\vec{v}',t) - \Sigma_f(\vec{r},\vec{v},t)\sum_{i=2}^{I}\left(\sum_{j=i}^{I}\frac{j!\check{c}_j(\vec{r},\vec{v},t)}{i!(j-i)!}\right)\left[-\int \mathrm{d}\vec{v}'\chi(\vec{v}\to\vec{v}')\mathcal{G}(z;\vec{r},\vec{v}',t)\right]^i, \tag{34}$$

$$\mathcal{G}(z;\vec{r},\vec{v},t_f) = \begin{cases} 1-z & \text{for } \vec{r},\vec{v}\in R \\ 0 & \text{for } \vec{r},\vec{v}\notin R \end{cases}$$

$$\mathcal{G}(z;\vec{r}_B,\vec{v},t) = 0, \quad \vec{r}\in\partial R, \quad \vec{e}_B\cdot\hat{\Omega} > 0,$$

where $\partial R$ is the surface of $R$ and $\vec{e}_B$ is the surface normal of $\partial R$. By taking successive derivatives of Eq. (34) with respect to $z$, solving for $\overline{n^k}$ at each step and evaluating at $z = 1$, we arrive at a general equation for the $k^{th}$ moment:

| $k$ | $S_k(\vec{r},\vec{v},t,\overline{n},\overline{n^2},\ldots,\overline{n^{k-1}})$ |
|---|---|
| 1 | 0 |
| 2 | $2\Lambda_2\langle\overline{n}\rangle^2$ |
| 3 | $6\langle\overline{n}\rangle[\Lambda_2\langle\overline{n^2}\rangle+\Lambda_3\langle\overline{n}\rangle^2]$ |
| 4 | $6\Lambda_2\langle\overline{n^2}\rangle^2+\langle\overline{n}\rangle[8\Lambda_2\langle\overline{n^3}\rangle+36\Lambda_3\langle\overline{n^2}\rangle\langle\overline{n}\rangle+24\Lambda_4\langle\overline{n}\rangle^3]$ |

**Table 13:** Neutron moment dependent source terms up to the fourth order moment.

$$\begin{aligned}\left(-\frac{1}{v}\frac{\partial}{\partial t}-\hat{\Omega}\cdot\nabla+\Sigma_t(\vec{r},\vec{v},t)\right)\overline{n^k}(\vec{r},\vec{v},t)=&\int \mathrm{d}\vec{v}'\Sigma_s(\vec{r},\vec{v}\rightarrow\vec{v}',t)\overline{n^k}(\vec{r},\vec{v}',t)\\&+\overline{\nu}\Sigma_f(\vec{r},\vec{v},t)\int \mathrm{d}\vec{v}'\chi(\vec{v}\rightarrow\vec{v}')\overline{n^k}(\vec{r},\vec{v}',t)\\&+S_k(\vec{r},\vec{v},t,\overline{n},\overline{n^2},\ldots,\overline{n^{k-1}}),\end{aligned}\tag{35}$$

with the final and boundary conditions given by

$$\overline{n^k}(\vec{r},\vec{v},t_f)=\begin{cases}1 & \text{for } \vec{r},\vec{v}\in R\\ 0 & \text{for } \vec{r},\vec{v}\notin R\end{cases}$$

$$\overline{n^k}(\vec{r}_B,\vec{v},t)=0,\quad \vec{r}\in\partial R,\quad \vec{e}_B\cdot\hat{\Omega}>0.$$

Where this is a standard adjoint transport equation for the $k^{th}$ moment of the neutron number with a source term, $S_k$, that is dependent on all the lower order moments of the population distribution. The first few moments are surmised in Table (13), where

$$\Lambda_i(\vec{r},\vec{v},t)=\Sigma_f(\vec{r},\vec{v},t)\sum_{j=i}^{\nu_m^f}\frac{j!}{i!(j-1)!}q_j^f,\tag{36}$$

and

$$\langle\overline{n^k}\rangle\equiv\langle\overline{n^k}\rangle(\vec{r},\vec{v},t)=\int \mathrm{d}\vec{v}'\chi(\vec{v}\rightarrow\vec{v}')\overline{n^k}(\vec{r},\vec{v}',t).\tag{37}$$

It is clear that Eq. (35) must be solved for all lower order moments in an ascending manner to obtain the $k^{th}$ moment of the distribution. These moments that are obtained are the moments of a single chain induced by a single neutron described by Eq. (32). To describe the population as a whole for an entire system, we must conduct another balance of probabilities for a system containing a random, constant singlet-emitting spontaneous fission source, $\mathcal{S}$, and relate each source event to the chain moments derived above. This will provide a methodology for determining the moments of the entire neutron population in a system. In performing said probability balance to find another Master equation, transforming that equation and taking successive derivatives, we can determine the moments of the distribution. The first four moments are:

- Mean:

$$\overline{N}=\int \mathrm{d}\vec{r}\int \mathrm{d}\vec{v}\int_0^{t_f}\mathrm{d}t\mathcal{S}(\vec{r},\vec{v},t)\overline{n}(\vec{r},\vec{v},t)\tag{38}$$

- Variance:

$$V_N=\int \mathrm{d}\vec{r}\int \mathrm{d}\vec{v}\int_0^{t_f}\mathrm{d}t\mathcal{S}(\vec{r},\vec{v},t)\overline{n^2}(\vec{r},\vec{v},t)\tag{39}$$

- Skewness:

$$s_N = \frac{1}{V_N^{3/2}} \int \mathrm{d}\vec{r} \int \mathrm{d}\vec{v} \int_0^{t_f} \mathrm{d}t \mathcal{S}(\vec{r},\vec{v},t)\overline{n^3}(\vec{r},\vec{v},t) \tag{40}$$

- Excess Kurtosis:

$$\kappa_N = \frac{1}{V_N^{2}} \int \mathrm{d}\vec{r} \int \mathrm{d}\vec{v} \int_0^{t_f} \mathrm{d}t \mathcal{S}(\vec{r},\vec{v},t)\overline{n^4}(\vec{r},\vec{v},t). \tag{41}$$

### 7.2 Cumulative Fission Moments Using Deterministic Transport

The moments of the cumulative fission number are derived in a similar fashion as those for the neutron number. Previous work has provided the first few moments of the cumulative fission numbers for supercritical media in a limited lumped model description [10], where it is desired to derive the moments as functions of time as well as phase space [11]. This is done by conducting a balance of probabilities in the first collision interval and, by taking a limiting case of the balance, we find a Master equation describing the temporal behavior of a fission chain produced by a single neutron arbitrarily introduced into the system. This will eventually lead to an adjoint transport-like equation for the $k^{th}$ moment of the cumulative fission number, $\overline{f^k}(\vec{r},\vec{v},t)$, of a single fission chain. We then incorporate a source and can find the moments of the fission number for an entire system.

Thus, we begin by stating the adjoint transport Master equations, as derived by Prinja [11], describing the cumulative fission PDF, $P_f(R,t_f;\vec{p},t)$, for there having occurred $f$ fissions within the system due to the introduction of a neutron into a region $R$ at a time $t$ that is earlier than the time of observation, $t_f$, such that $t < t_f$, with phase space coordinate $\vec{p} = (\vec{r}, E, \hat{\Omega})$:

$$\begin{aligned}\left[ -\frac{\partial}{\partial t} - v\hat{\Omega}\cdot\nabla + \lambda_t \right] P_f(R,t_f;\vec{p},t) &= \lambda_c \delta_{f,0} + \lambda_s \int \mathrm{d}E' \int \mathrm{d}\Omega' \tilde{f}(E\to E', \hat{\Omega}\cdot\hat{\Omega}') P_f(R,t_f;\vec{p}',t) \\ &+ \lambda_f \left[ q_0 \delta_{f,1} + \sum_{\nu=1}^{\nu_m} q_\nu \sum_{\substack{f_1+f_2+\ldots \\ +f_\nu = f-1}} \prod_{i=1}^{\nu} \int \mathrm{d}E_i \int \mathrm{d}\Omega_i \chi_\nu(E,\hat{\Omega}\to\{E_1,\hat{\Omega}_1,\ldots,E_\nu,\hat{\Omega}_\nu\}) P_{f_i}(R,t_f;\vec{p}_i,t) \right],\end{aligned} \tag{42}$$

with final and boundary conditions

$$P_f(R,t_f;\vec{p},t_f) = \delta_{f,0} = \begin{cases} 1 & \text{for } f = 0 \\ 0 & \text{for } f \neq 0, \end{cases}$$

$$P_f(R,t_f;\vec{p},t) = \delta_{f,0}, \quad \vec{r}\in\partial R, \quad \vec{e}_B\cdot\hat{\Omega} > 0.$$

Here $\vec{p}' = (\vec{r}, E', \hat{\Omega}')$ and $\vec{p}_i = (\vec{r}, E_i, \hat{\Omega}_i)$. Note the difference in notation from the previous section of this appendix; we are using the combination of $\hat{\Omega}$ and $E$ instead of the velocity $\vec{v}$ as well as reaction rates, $\lambda_x$, where $x$ is a particular reaction. We now introduce the generating function transform for the cumulative fission PDF:

$$G(\vec{p},t;t_f,z) = \sum_{f=0}^{\infty} z^f P_f(R,t_f;\vec{p},t), \tag{43}$$

where we are omitting the $R$ dependence for brevity in the ensuing equations. Also worth noting $z$ is a real variable restricted to the interval $[0,1]$ to ensure convergence of the series of Eq. (43). By multiplying Eq. (42) by $z^f$ and summing over all $f$, we condense the infinite set of master equations into a single equation of $G(\vec{p},t;t_f,z)$, consequentially producing an adjoint transport-like equation:

$$\begin{aligned}\left[ -\frac{\partial}{\partial t} - v\hat{\Omega}\cdot\nabla + \lambda_t \right] G(\vec{p},t;t_f,z) &= \lambda_c + \lambda_s \int \mathrm{d}E' \int \frac{\mathrm{d}\Omega'}{4\pi} \tilde{f}(E\to E', \hat{\Omega}\cdot\hat{\Omega}') G(\vec{p}',t;t_f,z) \\ &+ \lambda_f z \sum_{\nu=0}^{\infty} q_\nu \left[ \int \mathrm{d}E' \chi(E') \int \frac{\mathrm{d}\Omega'}{4\pi} G(\vec{p}',t;t_f,z) \right]^\nu.\end{aligned} \tag{44}$$

| $k$ | $S_k(\vec{p}, s\|t))$ |
|---|---|
| 1 | $\Lambda_0$ |
| 2 | $\Lambda_0 + 2\langle\overline{f}\rangle(\Lambda_1 + 2\Lambda_2\langle\overline{f}\rangle)$ |
| 3 | $\Lambda_0 + (3\Lambda_1 + 6\Lambda_2\langle\overline{f}\rangle)(\langle\overline{f}\rangle + \langle\overline{f^2}\rangle) + 6\Lambda_3\langle\overline{f}\rangle^3$ |
| 4 | $\Lambda_0 + \Lambda_1(4\langle\overline{f^3}\rangle + 6\langle\overline{f^2}\rangle + 4\langle\overline{f}\rangle) + \Lambda_2(4\langle\overline{f}\rangle[2\langle\overline{f^3}\rangle + 6\langle\overline{f^2}\rangle + 3\langle\overline{f}\rangle] + 6\langle\overline{f^2}\rangle^2)$ $+12\Lambda_3\langle\overline{f}\rangle^2(3\langle\overline{f^2}\rangle + 2\langle\overline{f}\rangle) + 24\Lambda_4\langle\overline{f}\rangle^4$ |

**Table 14:** Cumulative fission moment dependent source terms up to the fourth moment.

Equation (44) has the final condition for $t \to t_f$: $G(\vec{p}, t_f; t_f, z) = 1$, and the boundary condition $G(\vec{p}, t|t_f, z) = 1$, $\vec{r} \in \partial V$, $\vec{e}_B \cdot \hat{\Omega} > 0$. As was done in the previous section regarding the neutron numbers, we may take successive derivatives of $G$ with respect to $z$, evaluating at $z = 1$, we obtain the factorial moments of $P_f$,

$$\left.\frac{\partial^k G}{\partial z^k}\right|_{z=1} = \overline{f(f-1)\cdot\ldots\cdot(f-k+1)}. \tag{45}$$

Upon expanding and simplifying the $k^{th}$ derivative evaluated at unity of Eq. (45) applied to Eq. (44), we obtain an adjoint transport equation for the $k^{th}$ moment of the cumulative fission PDF, $\overline{f^k}(\vec{p}, t; t_f)$, for a fission chain induced by a single initiating neutron:

$$\begin{aligned}\left[-\frac{\partial}{\partial t} - v\hat{\Omega}\cdot\nabla + \lambda_t\right]\overline{f^k}(\vec{p}, t; t_f) = \quad & \lambda_s \int \mathrm{d}E' \int \frac{\mathrm{d}\Omega'}{4\pi} \tilde{f}(E \to E', \Omega\cdot\Omega')\overline{f^k}(\vec{p}', t; t_f) \\ & + \lambda_f \overline{\nu} \int \mathrm{d}E \chi(E) \int \frac{\mathrm{d}\Omega'}{4\pi} \overline{f^k}(\vec{p}', t; t_f) + S_k(\vec{p}, t, \overline{f}, \overline{f^2}, \ldots, \overline{f^{k-1}}),\end{aligned} \tag{46}$$

where $S_k$ is a source term that is a function of all lower order fission moments and the first few are defined in Table (14). Due to this dependence on all of the lower order moments, one must solve for every lower order moment in an increasing unidirectional manner. Note that $\Lambda$ is defined by Eq. (36) and $\langle\cdot\rangle$ denotes integration over all out-scatter energies, such that

$$\langle\overline{f^k}\rangle \equiv \langle\overline{f^k}\rangle(\vec{p}, t) = \int \mathrm{d}E' \chi(E \to E')\overline{f^k}(\vec{p}', t). \tag{47}$$

Thus far, we have not considered systems with a spontaneous fission source, rather we were not able to incorporate SF into the initial formulation, $S(\vec{p}, t) = \mathcal{S}(t)w(\vec{p})$, assumed to be separable in phase space and time. The source magnitude is carried by $\mathcal{S}(t)$ and, therefore, $\int \mathrm{d}\vec{p} w(\vec{p}) = 1$. We formulate an adjoint master equation for $P_f^{(S)}(R, t; s)$, the probability of a fission occurring in $R$ at time $t$ due to a source event at time $s$, such that $s < t \leq t_f$. The fission source PDF satisfies the following partial differential equation:

$$-\frac{\partial P_f^{(S)}}{\partial s} = -\mathcal{S}(s)P_f^{(S)}(R, t; s) + \mathcal{S}(s) \sum_{f_1+f_2=f-1} \int \mathrm{d}\vec{p} w(\vec{p}) P_{f_1}(R, t; \vec{p}, s) P_{f_2}^{(S)}(R, t; s), \tag{48}$$

where it is clear that $P_f^{(S)}$ is implicitly a function of $P_{f_i}$, the probability of the $i^{th}$ fission chain propagating to the point in space-time $s$. As has been done for all previously encountered Master equations within this document, we apply the source generating function, $G^{(S)}(R, t; s, z)$ and solve ascertained ODE by separation of variables. The solution of generating function transport equation with a source,

$$G^{(S)}(R, t; s_0, z) = \exp\left[-\int_{s_0}^{t} \mathrm{d}s \mathcal{S}(s) \int \mathrm{d}\vec{p} w(\vec{p}) G(R, t; \vec{p}, s, z)\right], \tag{49}$$

can be differentiated with respect to $z$ and evaluated at unity to obtain the factorial moments of the fission chains induced by source events. Finally, we may arrive at the moments of the entire system; the first four moments are defined as:

- Mean:

$$\overline{F} = \int_0^{t_f} \mathrm{d}s\mathcal{S}(s) \int \mathrm{d}\vec{p}w(\vec{p})\overline{f}(\vec{p},s) \tag{50}$$

- Variance:

$$V_F = \int_0^{t_f} \mathrm{d}s\mathcal{S}(s) \int \mathrm{d}\vec{p}w(\vec{p})\overline{f^2}(\vec{p},s) \tag{51}$$

- Skewness:

$$s_F = \frac{1}{V_F^{3/2}} \int_0^{t_f} \mathrm{d}s\mathcal{S}(s) \int \mathrm{d}\vec{p}w(\vec{p})\overline{f^3}(\vec{p},s) \tag{52}$$

- Excess Kurtosis:

$$\kappa_F = \frac{1}{V_F^2} \int_0^{t_f} \mathrm{d}s\mathcal{S}(s) \int \mathrm{d}\vec{p}w(\vec{p})\overline{f^4}(\vec{p},s) \tag{53}$$

**References**


[1] Fichtl, E. and Baker, R., "Computing the Moments of the Neutron Population Using Deterministic Neutron Transport." International Conference on Mathematics and Computational Methods Applied to Nuclear Science & Engineering (M&C 2013).

[2] Sweezy, J., "Collision of Physics and Software in the Monte Carlo Application Toolkit (MCATK)." Presentation to West Point Physics Dept. Staff. Lecture. LA-UR-16-20300.

[3] Adams, T., Nolen, S., Sweezy, J., Zukaitis, A., Campbell, J., Goorley, T., Greene, S., and Aulwes, R., "Monte Carlo Application ToolKit (MCATK)." Annals of Nuclear Energy 82 (2015): 41-47. Web. LA-UR-13-27979.

[4] Alcouffe, R., Baker, R., Dahl, J., Fichtl, E., Turner, S., Ward, R., and Zerr, R., "PARTISN: A Time-Dependent, Parallel Neutral Particle Transport Code System." Manual. Los Alamos National Laboratory Report LA-UR-08-07258.

[5] Lewis, E., and Miller, W., "Computational Methods of Neutron Transport". New York: Wiley, 1984.

[6] Enqvist, A., Pazsit I., and Pozzi, S., "The Number Distribution of Neutrons and Gamma Photons Generated in a Multiplying Sample." Nuclear Instruments and Methods: Accelerators, Spectrometers, Detectors and Associated Equipment 566.2, 598-608, (2006).

[7] Bell, G., "On the Stochastic Theory of Neutron Transport," Nuclear Science and Engineering, 21, pp. 390-401 (1965).

[8] Pal, L., "On the Theory of Stochastic Processes in Nuclear Reactors," Nuovo Cimento, 7, pp. 25-42 (1958).

[9] Prinja, A. and Souto, F., "Probability Distributions for Neutron Multiplying Systems without Delayed Neutrons," Los Alamos National Laboratory report LA-UR 09-07886 (2009).

[10] Fichtl, Erin D., and Anil K. Prinja. "The Asymptotic Probability Distribution of Fission Numbers in a Multiplying System."

[11] Prinja, Anil K. "A Stochastic Theory of Number Distributions of Fissions in a Multiplying Assembly." Letter to Erin Fichtl. N.d. MS. Albuquerque, New Mexico.